Bolt Beranek and Newman Inc.

1300 North 17th Street, Suite 400, Arlington, VA 22209

Technical Memorandum W804

DEPENDENCE ON APERTURE ANGLE OF ARRAY GAIN AGAINST FLOW NOISE FOR CYLINDRICAL AND SPHERICAL ARRAYS OF DIRECTIONAL ELEMENTS

July 1983

H. Cox
J.M. Steele

DARPA Order No. 4462

Contract No. N00014-83-C-0167

Submitted to:

Office of Naval Research
800 N. Quincy Street
Arlington, VA 22217

Attention: James Webster, Code 220

The views and conclusions contained in this document are those of the authors and should not be interpreted as necessarily representing the official policies, either expressed or implied, of the Defense Advanced Research Projects Agency or the U.S. Government.

UNCLASSIFIED

SECURITY CLASSIFICATION OF THIS PAGE (When Data Entered)

REPORT DOCUMENTATION PAGE	READ INSTRUCTIONS BEFORE COMPLETING FORM
1. REPORT NUMBER	2. GOVT ACCESSION NO. AD-A131144 / 3. RECIPIENT'S CATALOG NUMBER
4. TITLE (and Subtitle) Dependence on aperture angle of array gain against flow noise for cylindrical and spherical arrays of directional elements	5. TYPE OF REPORT & PERIOD COVERED Technical / 6. PERFORMING ORG. REPORT NUMBER Technical Memo No. W804
7. AUTHOR(S) H. Cox, J. M. Steele	8. CONTRACT OR GRANT NUMBER(S) N00014-83-C-0167
9. PERFORMING ORGANIZATION NAME AND ADDRESS Bolt Beranek and Newman Inc. 1300 North 17th Street Arlington, Virginia 22209	10. PROGRAM ELEMENT PROJECT TASK AREA & WORK UNIT NUMBERS
11. CONTROLLING OFFICE NAME AND ADDRESS Office of Naval Research 800 North Quincy Street Arlington, Virginia 22217	12. REPORT DATE July 1983 / 13. NUMBER OF PAGES 42
14. MONITORING AGENCY NAME & ADDRESS (if different from Controlling Office) Defense Advanced Research Projects Agency 1400 Wilson Boulevard Arlington, Virginia 22209	15. SECURITY CLASS. (of this report) Unclassified / 15a. DECLASSIFICATION/DOWNGRADING SCHEDULE N/A
16. DISTRIBUTION STATEMENT (of this Report) Unlimited	
17. DISTRIBUTION STATEMENT (of the abstract entered in Block 20, if different from Report)	
18. SUPPLEMENTARY NOTES	
19. KEY WORDS (Continue on reverse side if necessary and identify by block number) Arrays, Array Gain, Cylindrical Array, Spherical Arrays, Flow Noise	

20. ABSTRACT (Continue on reverse side if necessary and identify by block number)

When receiving arrays are placed on air backed structures in water, the effect of the structure or baffle is to alter the response of the hydrophones from their free field characteristics. The exact response characteristics are complicated and frequency dependent. Typically the response is reduced near grazing incidence. When a beam is formed for maximum response in a selected direction, increasing the aperture to include elements for which the selected beam direction is near grazing, ——> cont.

DD FORM 1 JAN 73 1473 EDITION OF 1 NOV 65 IS OBSOLETE

UNCLASSIFIED

SECURITY CLASSIFICATION OF THIS PAGE (When Data Entered)

20.

is inefficient in increasing array signal gain and may actually lead to a loss in signal-to-noise ratio. The array gain dependence upon aperture angle for cylindrical and spherical arrays has been presented for parametric families of effective element directivities. Both uniform and optimum shadings have been considered. Results have been presented in the form of parametric curves which can be used in system design tradeoffs. These results may be used to fit structural analyses and experimental data for various ACSAS candidate designs.

The use of elements when their signal response is low such as near grazing incidence has been shown to provide little additional gain against flow noise. For the cylindrical array it has been found that increasing the aperture angle beyond about 120 degrees provides less than 1 dB additional gain. Therefore economic and other system considerations such as D/E steering should be the primary factors in extending the aperture beyond 120°.

For the spherical array increasing aperture angle has about twice the payoff as for the cylindrical array since both azimuthal and vertical resolution depend on the aperture angle. Of course twice a small number may be still very small. In practice, since the sphere may be used over a wide range of azimuths and must have elements for those azimuths, it may be desirable to take advantage of those elements by increasing the aperture in the horizontal dimension without adding elements near the top and bottom.

Technical Memorandum W804

DEPENDENCE ON APERTURE ANGLE OF ARRAY GAIN AGAINST FLOW NOISE FOR CYLINDRICAL AND SPHERICAL ARRAYS OF DIRECTIONAL ELEMENTS

July 1983

H. Cox
J.M. Steele

DARPA Order No. 4462

Contract No. N00014-83-C-0167

Submitted to:

Office of Naval Research
800 N. Quincy Street
Arlington, VA 22217

Attention: James Webster, Code 220

Submitted by:

Bolt Beranek and Newman Inc.
1300 North 17th Street, Suite 400
Arlington, VA 22209

A

TABLE OF CONTENTS

LIST OF FIGURES

LIST OF FIGURES (continued)

LIST OF TABLES

1. INTRODUCTION

The ACSAS array will consist of a large number of elements mounted on a complicated structure involving the submarine hull, ballast tanks and the outer and inner decouplers. The effect of the structure or baffle will be to alter the response of the hydrophone elements from their free field response. In general we expect maximum response near normal incidence and a reduced response near grazing incidence.

The inclusion of elements as part of the aperture used to steer a beam in a direction for which sound has near grazing incidence to those elements is inefficient and can lead to beam pattern degradation and even loss of signal-to-noise ratio.

In this technical memorandum we examine the signal-to-noise ratio aspect of using elements far from normal incidence. We examine two geometries: a cylinder, representative of the side mounted portion of the ACSAS array, and a spherical cap, representative of the bow area. A horizontally oriented cylinder with sound arriving from broadside in the horizontal plane is illustrated in Figure 1. Elements near the top and bottom of the cylinder have a near grazing incidence while elements near the center line have a near normal incidence. The question of interest is: "How does the signal-to-noise ratio or array gain vary as the aperture angle is increased to include elements with near grazing incidence?" The same question is of importance for a spherical cap aperture.

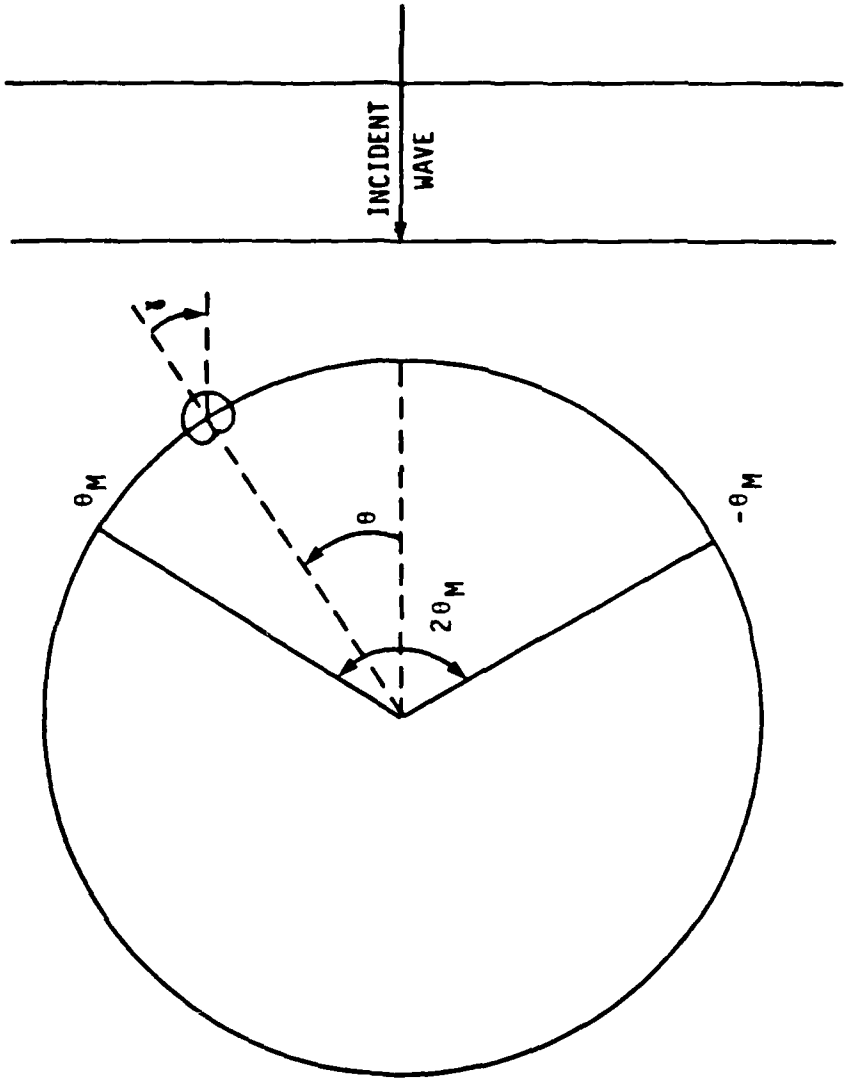

FIGURE 1 Cylindrical Geometry

Various parametric families of element directivities will be considered. This provides insight concerning the sensitivity of array performance to effective element directivity. It also facilitates the use of the results for element directivities obtained by measurement or structural acoustic calculations, since one can approximate by selection of the parametric directivities which most closely match or bracket the data.

Since aperture angle is a significant system tradeoff parameter and may be an important cost consideration, our goal is to provide results in a form which can be used directly in system tradeoffs.

2. ELEMENT DIRECTIVITY

2.1 Cosine and Cardiod Family

The determination of the directional response of a hydrophone element on realistically representative structures is a complex problem in structural acoustics. Analytic predictions by several methods are being pursued for various ACSAS candidate designs under a separate task. We will proceed parametrically by considering a significant range of element directivities in order to permit a subsequent fit of these calculations to structural acoustic analysis and experimental data.

Let $b(\gamma)$ be the directional amplitude response of an element where γ is measured from the normal to the face of the element. We assume that all elements have the same directional response when measured from the appropriate normal. For simplicity we assume a dependence on only a single angle γ. For the cylinder this is adequate since we examine the case of sound arriving from broadside. For the sphere it is reasonable because of symmetry. The range of angles $|\gamma| \leq \frac{\pi}{2}$ is of primary interest.

The following element directivities will be considered as the cosine and cardiod family.

I	$b(\gamma) = 1 = (\cos\gamma)^0, \quad \lvert\gamma\rvert \le \frac{\pi}{2}$	omnidirectional
II	$b(\gamma) = (\cos\gamma)^{1/4}, \quad \lvert\gamma\rvert \le \pi/2$	$(\text{cosine})^{1/4}$
III	$b(\gamma) = (\cos\gamma)^{1/2}, \quad \lvert\gamma\rvert \le \pi/2$	$(\text{cosine})^{1/2}$
IV	$b(\gamma) = \cos\gamma, \quad \lvert\gamma\rvert \le \pi/2$	cosine
V	$b(\gamma) = \frac{1}{2}(1 + \cos\gamma)$	cardiod
VI	$b(\gamma) = \left[\frac{1}{2}(1 + \cos\gamma)\right]^2$	$(\text{cardiod})^2$

The cardiod patterns which extend into the shadow region $\pi/2 \le \lvert\gamma\rvert \le \pi$ allow for some diffraction and may be more realistic close to grazing. The most severe directionality is cosine (IV). Figure 2 presents plots of the various element directivities on a dB scale (20 log b). The responses at selected angles is presented in Table 1. For small angles the relationship

$$(\cos\gamma)^{1/2} \approx \frac{1}{2}(1 + \cos\gamma) \qquad (1)$$

leads to a similarity between responses III and V, as well as IV and VI.

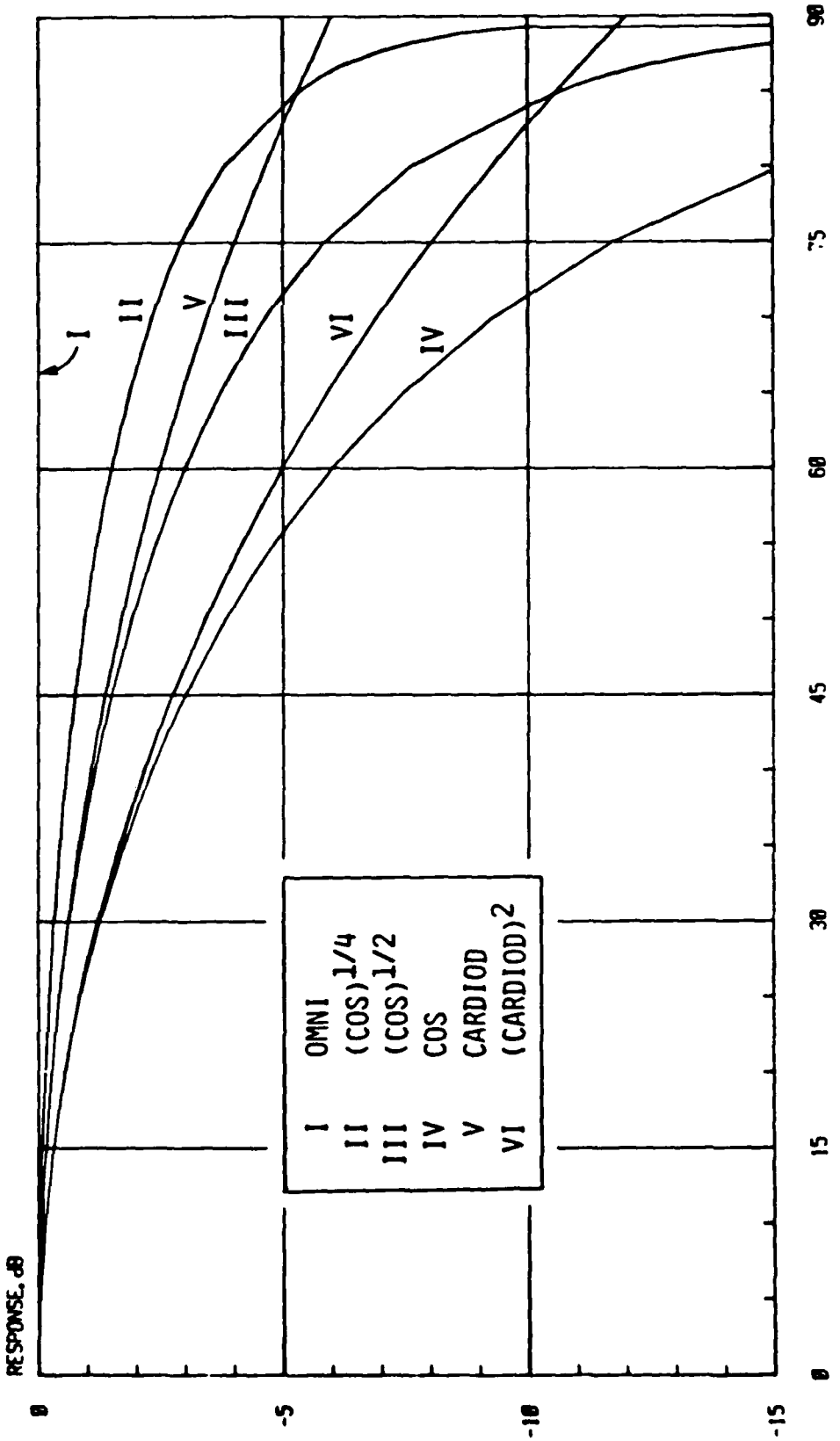

FIGURE 2 Element Response (dB)

TABLE 1. DIRECTIONAL RESPONSE 20 log b(Y) FOR SELECTED ANGLES

ANGLE	30°	45°	60°	75°	85°	90°
DIRECTIVITY	dB	dB	dB	dB	dB	dB
I omni	0	0	0	0	0	0
II $(\cos)^{1/4}$	-0.31	-0.75	-1.50	-2.94	-5.30	$-\infty$
III $(\cos)^{1/2}$	-0.62	-1.50	-3.01	-5.87	-10.60	$-\infty$
IV cos	-1.25	-3.01	-6.02	-11.74	-21.20	$-\infty$
V cardiod	-0.60	-1.38	-2.50	-4.02	-5.29	-6.02
VI $(\text{cardiod})^2$	-1.20	-2.75	-5.00	-8.04	-10.59	-12.04

2.2 Infinite Flat Plate

A standard problem for which a simple analytic expression for element directivity is available is a hydrophone on the face of an air backed infinite flat plate below the critical frequency for flexural waves. Results for a cylindrical or spherical shell may be anticipated to go asymptomatically to the flat plate solution as frequency increases if there is adequate internal damping of the shell.

For an incident monochromatic plane wave of amplitude P_{inc} at an angle of incidence γ a hydrophone on the face of the plate will sense a complex pressure P_{tot} which is the sum of the incident and reflected waves

$$P_{tot} = \frac{i\ 2(\omega m/\rho c)\cos\gamma}{1 + i\ (\omega m/\rho c)\cos\gamma}\ P_{inc} \qquad (2)$$

where $(i\omega m)$ is the normal specific acoustic impedence of the surface, m is the mass per unit area of the plate and ρc is the impedence of the fluid (water) in which the incident wave is propagating.

Three quantities pertaining to the response are of interest. The first is the sensitivity at normal incidence.

$$A = (2\alpha)/(1 + \alpha^2)^{1/2} \qquad (3)$$

where α is the ratio of impedence $(\omega m/\rho c)$. The second is the normalized directional amplitude response

$$b(\gamma) = \frac{(1 + \alpha^2)^{1/2}\cos\gamma}{(1 + \alpha^2\cos^2\gamma)^{1/2}} \qquad (4)$$

The third is the phase of the response

$$\phi(\gamma) = \pi/2 - \tan^{-1}(\alpha \cos \gamma) \tag{5}$$

Equation (2) may than be written as

$$P_{tot} = A\, b(\gamma) \exp(i\,\phi(\gamma))\, P_{inc} \tag{6}$$

The quantities A, $b(\gamma)$ and $\phi(\gamma)$ are plotted in Figures (3), (4) and (5) respectively.

The curves of Figure 4 are very similar to those of Figure 1. Table 2 which is analogous to Table 1 presents $b(\gamma)$ for various values of the impedance ratio α. Cosine and $(\text{cosine})^{\frac{1}{2}}$ are also listed for comparison. It is clear that for small α, Eq. (4) is approximately a cosine directivity.

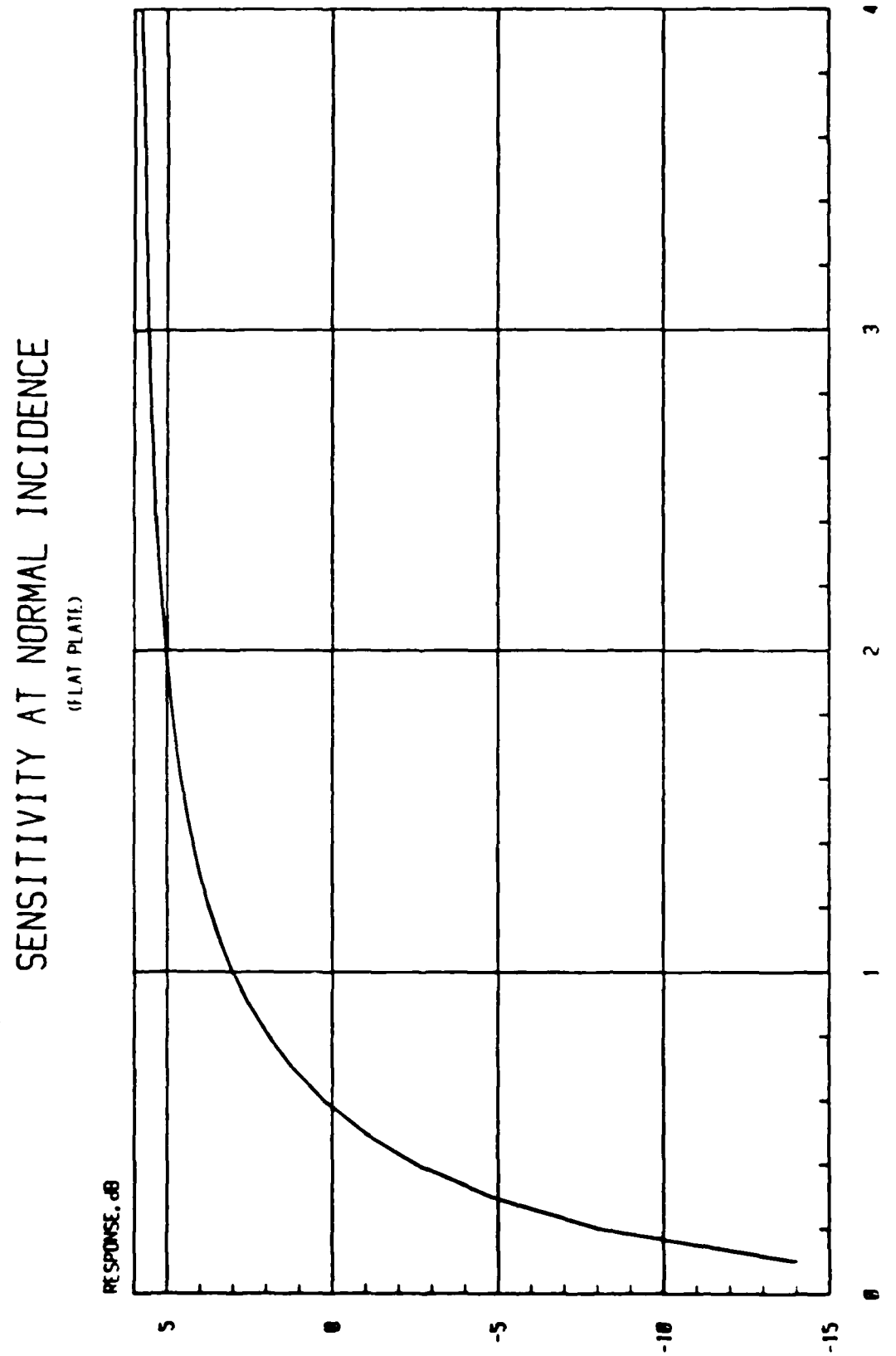

FIGURE 3 Sensitivity of Element on a Zero Impedance Backed Infinite Flat Plate to Sound at Normal Incidence (dB)

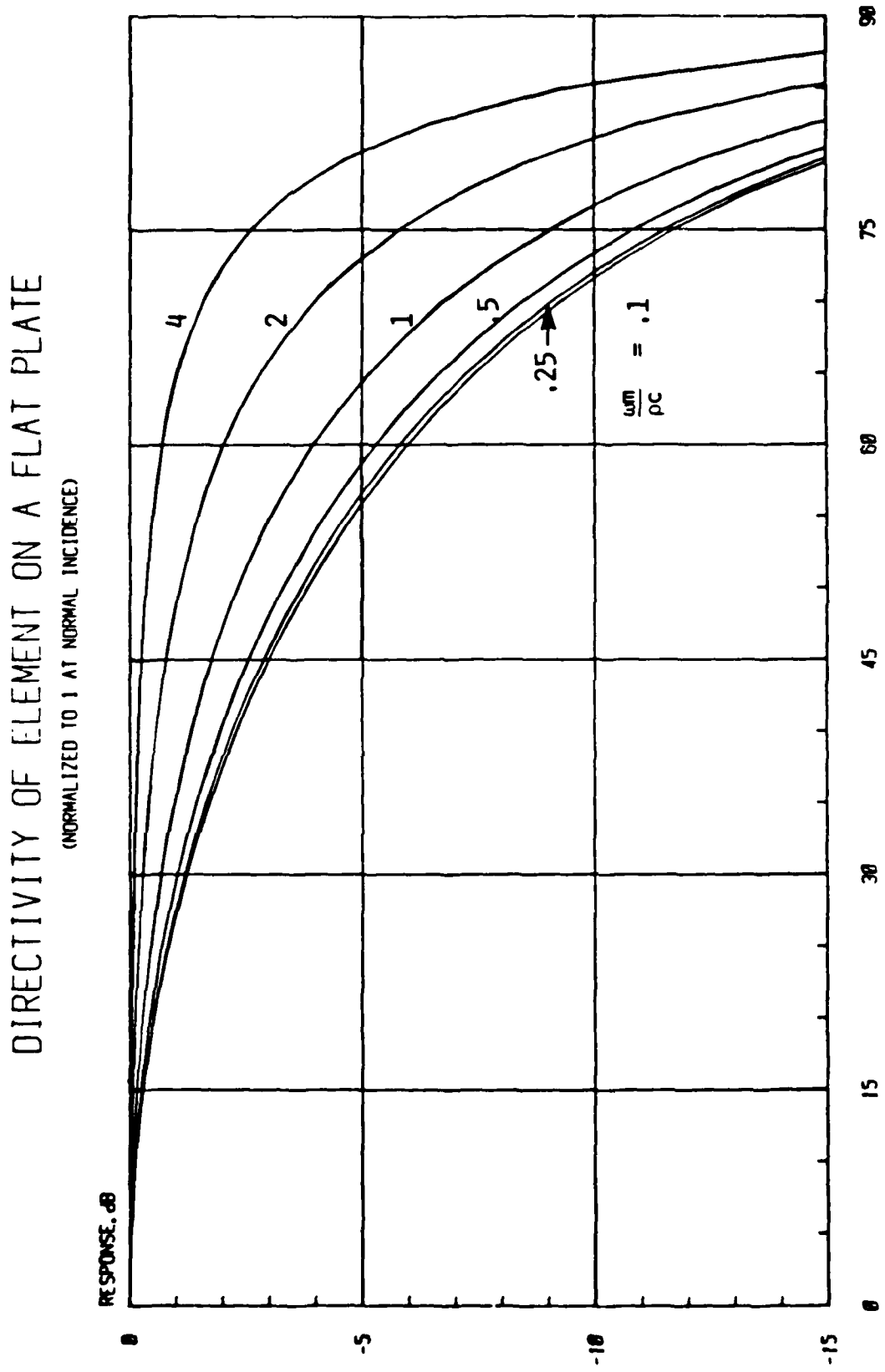

FIGURE 4 Directivity of Element on a Zero Impedance Backed Infinite Flat Plate (dB)

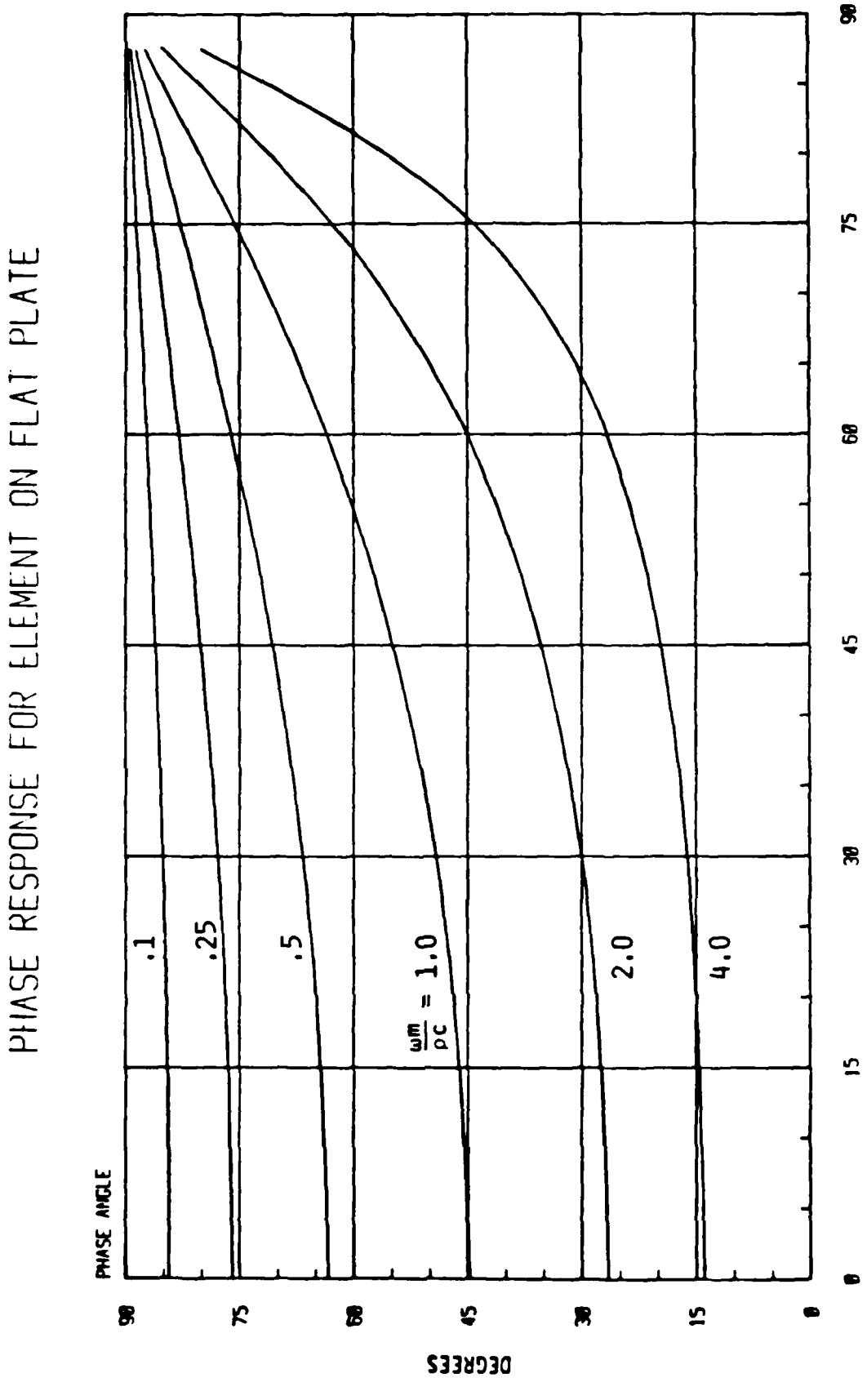

FIGURE 5 Phase Response

TABLE II. COMPARISON OF DIRECTIONAL RESPONSE 20 log b(Y) OF ELEMENT ON FLAT PLATE AT VARIOUS VALUES OF $\alpha = \omega m/\rho c$ WITH COSINE AND $(\text{COSINE})^{\frac{1}{2}}$ RESPONSE

ANGLE	30	45	60	75	85
DIRECTIVITY	dB	dB	dB	dB	dB
α = 0.1	-1.24	-2.99	-5.99	-11.70	-21.15
0.25	-1.19	-2.88	-5.82	-11.49	-20.93
0.5	-1.03	-2.55	-5.31	-10.84	-20.23
1.0	-0.67	-1.76	-3.98	-9.01	-18.22
2.0	-0.28	-0.79	-2.04	-5.78	-14.33
IV cos	-1.25	-3.01	-6.02	-11.74	-21.20
III $(\cos)^{\frac{1}{2}}$	-0.62	-1.50	-3.01	-5.87	-10.60

The strong similarity between the curves of Figure 2 with those of Figure 4 is noteworthy.

Even though diffraction and resonant elastic waves complicate the picture for a cylinder and a sphere, we expect the infinite flat plate results to be a reasonable approximation at sufficiently high frequencies. Consider the cylinder. When the circumference of the cylinder is larger than an acoustic wavelength in water ($Ka > 1$) diffraction will be of reduced importance. For a 20 foot radius cylinder in water $Ka = 1$ at about 40 Hz. Curvature will be of reduced importance in the propagation characteristics of free waves in a cylindrical shell for frequencies above the "ring frequency," the frequency for which the circumference of the cylinder is equal to a compressional wavelength in the shell. For a steel cylinder of 20 foot radius the ring frequency is about 160 Hz.

A finite extent structure may be adequately modeled for many purposes by an infinite extent structure for frequencies sufficiently high and/or damping sufficiently large that there is modal overlap - that is, the bandwidth of single resonant mode exceeds the typical frequency interval between modes. This criterion is equivalent to the requirement that there be significant (i.e., > 6 dB) spatial attenuation of free waves across the extent of the structure. For 1" thick 20' radius shell, a $\eta = 0.01$ structural loss factor is sufficient to yield 6 dB attenuation of a flexural wave in a circumference for frequencies in excess of 300 Hz. Thus the flat plate results will adequately describe cylindrical response in the illuminated sector not too close to the shadow line (i.e., local grazing) for the above example cylinder above ring frequency if it is reasonably well damped.

3. ARRAY GAIN

3.1 Cylindrical Array

Consider the horizontal cylinder shown in Figure 1 with the signal arriving from broadside in the horizontal plane. The aperture covers the section of the cylinder $|\theta| \leq \theta_M$ so that θ_M is the aperture half-angle. The noise is assumed to be spatially uncorrelated. For our purpose, this is an adequate model for flow noise. We will investigate the effect on array gain of varying the aperture angle $2\theta_M$.

The aperture is assumed to be densely covered with elements of the same directivity $b(\Upsilon)$. Let $a(\theta)$ be the amplitude shading function applied to the aperture. We assume that the elements are properly phased for maximum response in the signal direction. As indicated in Figure 4 such phasing includes both the plane wave time-delay and the variation in phase across the aperture introduced by the baffle.

Then the array gain per unit length along the cylinder of radius R is

$$G(\theta_M) = \frac{\left[2R \int_0^{\theta_M} a(\theta)\ b(\theta)\ d\theta\right]^2}{2R \int_0^{\theta_M} a^2(\theta)\ N(\theta)\ d\theta} \qquad (7)$$

where $N(\theta)$ is the normalized uncorrelated noise density. It is assumed to be unity for a uniform noise field. This assumption simply means that the noise level does not vary with position in the aperture.

For uniform shading ($a(\theta) = 1$) and uniform uncorrelated noise ($N(\theta) = 1$), Eq. (7) reduces to

$$G_u(\theta_M) = \frac{2R}{\theta_M} \left[\int_o^{\theta_M} b(\theta)\, d\theta \right]^2 \tag{8}$$

where the subscript u denotes uniform shading ($a(\theta) = 1$).

The shading which maximizes array gain is the Eckart shading

$$a_o(\theta) = b(\theta) \Big/ \sqrt{N(\theta)} \tag{9}$$

which for uniform noise reduces to

$$a_o(\theta) = b(\theta) \tag{10}$$

The subscript o denotes optimum shading. Notice that the optimum shading for maximizing signal-to-noise ratio is identical to the element directivity.

Elements are weighted in proportion to their signal response. Thus elements with near grazing incidence and low signal response are given very small weighting. Substituting from Eq. (10) into Eq. (7) gives the following expression for optimum array gain per unit length in a uniform uncorrelated noise field

$$G_o(\theta_M) = 2R\int_o^{\theta_M} b^2(\theta)\, d\theta \quad . \tag{11}$$

It is noteworthy that $G_o(\theta_M)$ increases monotonically with θ_M but $G_u(\theta_M)$ may not. For many of the element directivities under consideration it is possible to integrate Eq. (8) and Eq. (11) analytically to obtain closed form expressions for $G_u(\theta_M)$ and $G_o(\theta_M)$. These results are summarized in Table 3.

The maximum array gain occurs for the omni-directional element $b(\gamma) = 1$. This maximum array gain per unit length is equal to πR and is achieved at $\theta_M = \pi/2$ when the full half cylinder is used for the aperture. In this case uniform shading is optimum.

Figures 6 through 9 present graphs of normalized array gain per unit length.

$$10 \log [G(\theta_M)/\pi R]$$

TABLE 3. ARRAY GAIN PER UNIT LENGTH FOR UNIFORM AND OPTIMUM SHADING

$b(\Upsilon)$	$G_u(\theta_M) = \frac{2R}{\theta_M}\left[\int_0^{\theta_M} b(\xi)\, d\xi\right]^2$	$G_o(\theta_M) = 2R\int_0^{\theta_M} b^2(\xi)\, d\xi$
1	$2\theta_M R$	$2\theta_M R$
$\left[\cos(\Upsilon)\right]^{1/4}$	See Figure 7	See Figure 6
$\left[\cos\Upsilon\right]^{1/2}$	See Figure 7	$2R\sin\theta_M$
$\cos\Upsilon$	$\frac{2\sin^2\theta_M}{\theta_M} R$	$\left[\theta_M + \frac{1}{2}\sin 2\theta_M\right] R$
$\frac{1+\cos\Upsilon}{2}$	$\left[\frac{\theta_M + \sin\theta_M}{2\theta_M}\right] R$	$\left[\frac{3}{4}\theta_M + \sin\theta_M + \frac{1}{8}\sin 2\theta_M\right] R$
$\left[\frac{1+\cos\Upsilon}{2}\right]^2$	$R\frac{2}{\theta_M}\left[\frac{3}{8}\theta_M + \frac{\sin\theta_M}{2} + \frac{\sin 2\theta_M}{16}\right]^2$	$\left[\frac{35}{64}\theta_M + \frac{7}{8}\sin\theta_M + \frac{7}{32}\sin 2\theta_M + \frac{1}{24}\sin 3\theta_M + \frac{1}{256}\sin 4\theta_M\right] R$
$\left[\frac{1+\bullet^2}{\frac{1}{\cos^2\gamma}+\bullet^2}\right]^{1/2}$	See Figure 9	See Figure 8

This normalization clearly shows the effect of element directivity on reducing gain against uncorrelated noise.

Figure 6 presents results for optimum shading and various directivities of the cosine and cardiod family. The maximum gain at $\theta_M = 90^\circ$ for cosine directivity is 3 dB below that for omnidirectional directivity. For all cases except omnidirectional, the additional gain achieved by increasing θ_M from 60 to 90 degrees is less than 1 dB. For small angles the gain is insensitive to the element directivity and increases by 3 dB per doubling of θ_M.

Figure 7 differs from Figure 6 in that uniform shading is used. The curves are very similar to the curves of Figure 6 except that for severe directivities such as cosine, the gain is reduced when the aperture is increased beyond a certain point. Adding elements with low signal-to-noise ratio reduces gain if these elements receive too high a weighting. Even in the most severe case the corresponding curves of Figure 6 and Figure 7 differ by less than 1 dB at $\theta_M = 90^\circ$ and by less than 0.2 dB at $\theta_M = 60^\circ$.

Figures 8 and 9 present corresponding results for "flat plate" element directivities. They closely resemble Figures 6 and 7 and lead to the same observations.

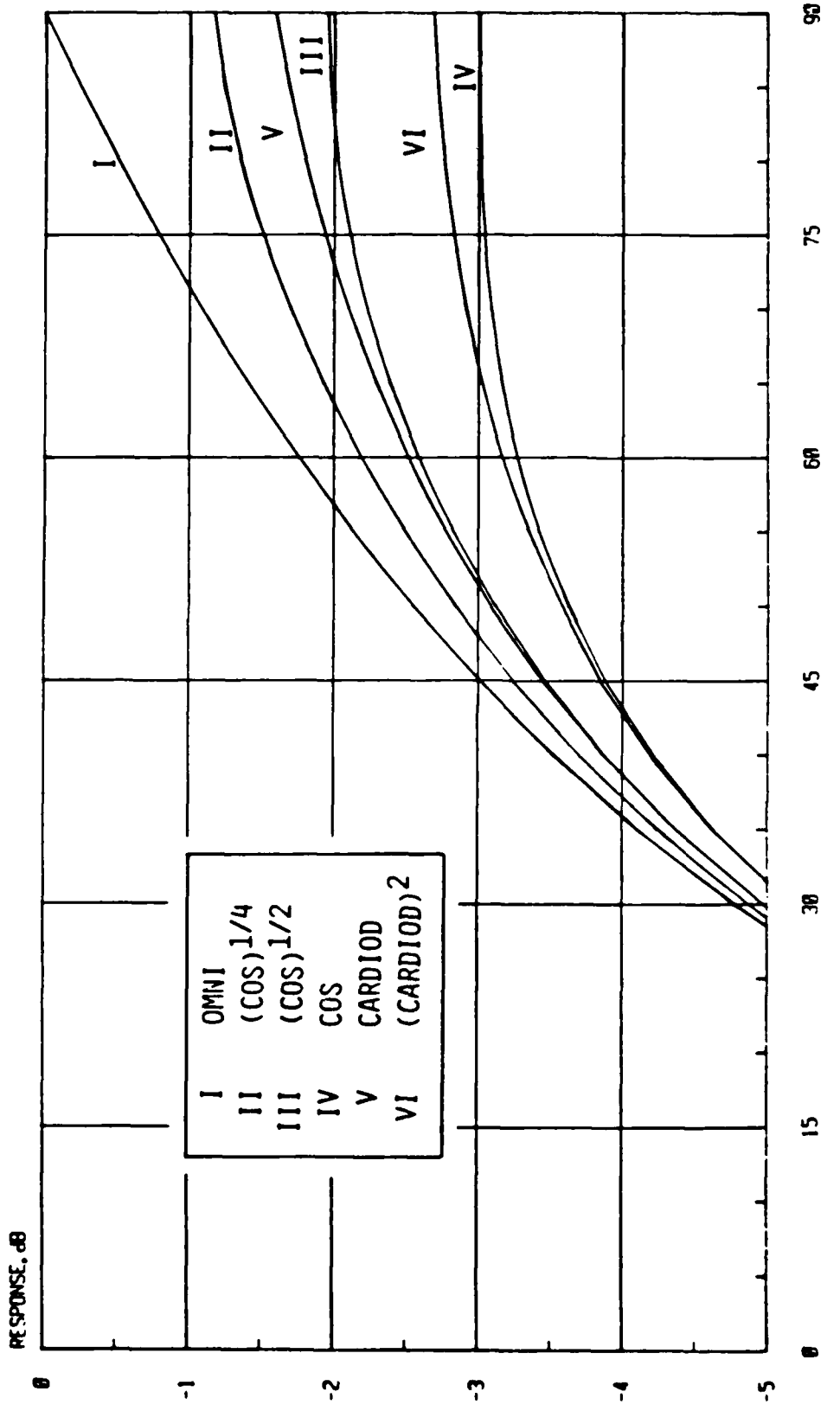

FIGURE 6 Normalized Array Gain Per Unit Length for Optimum Shading

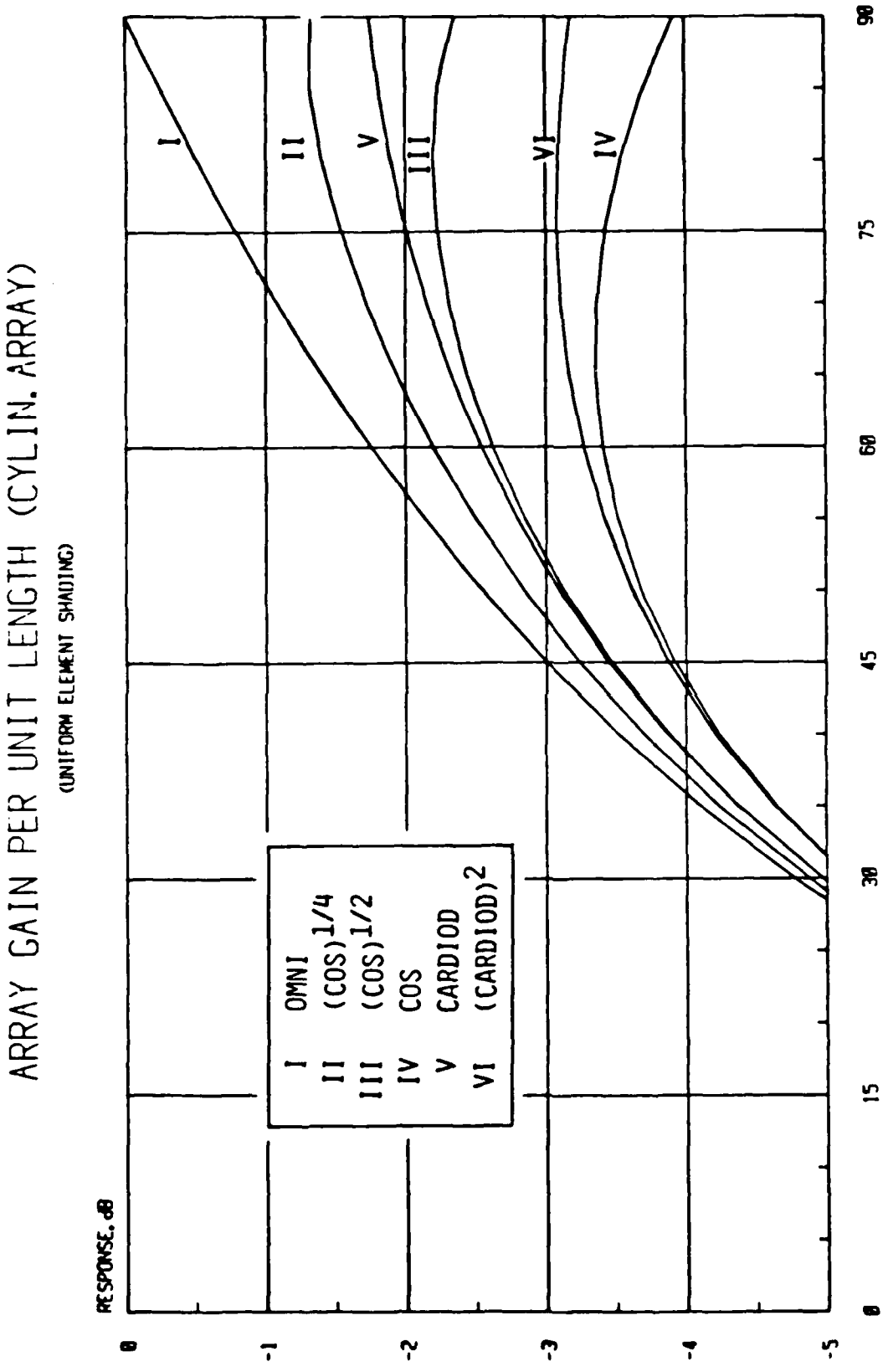

FIGURE 7 Normalized Array Gain Per Unit Length for Uniform Shading

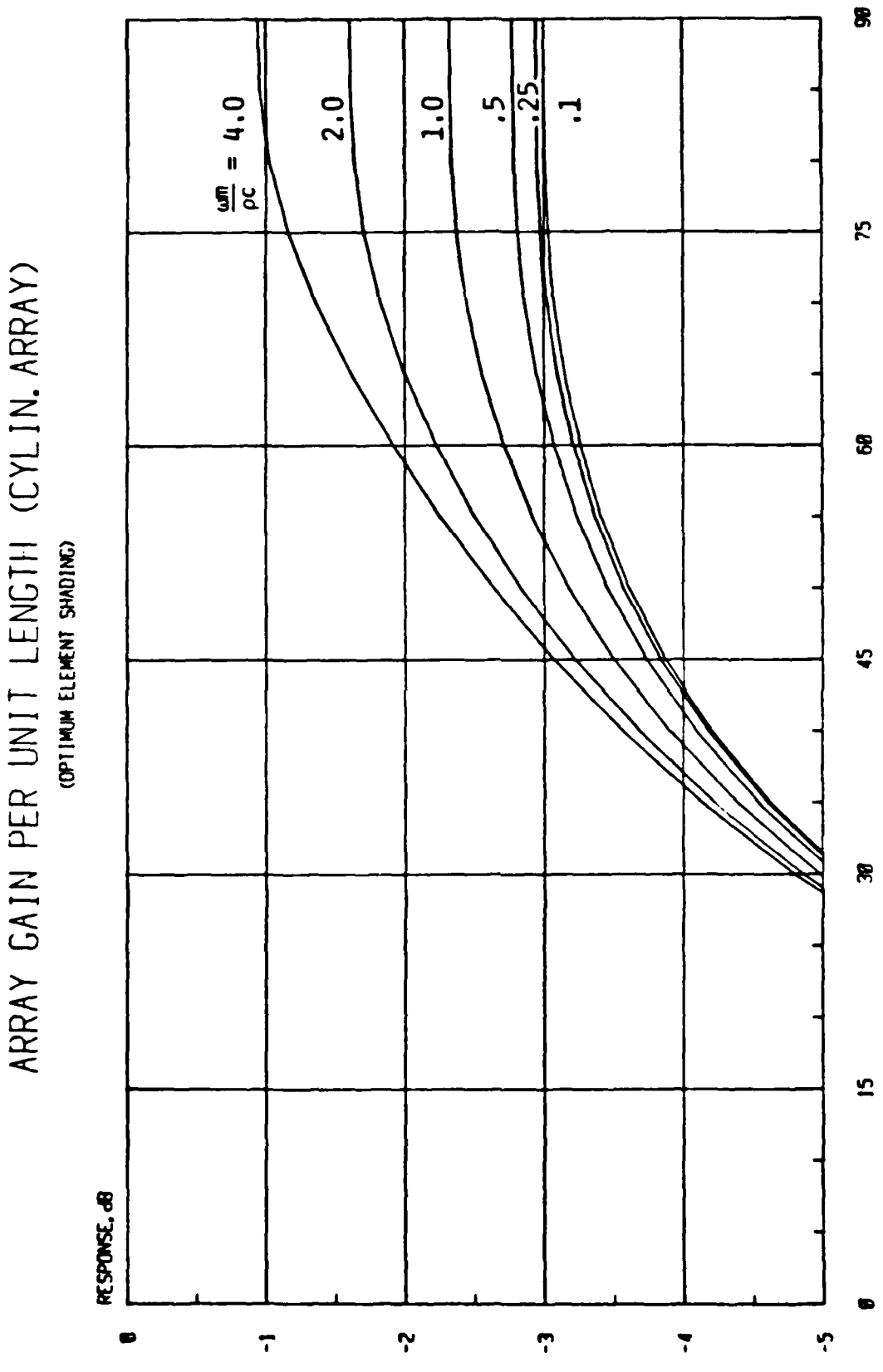

FIGURE 8 Normalized Array Gain Per Unit Length for Optimum Shading

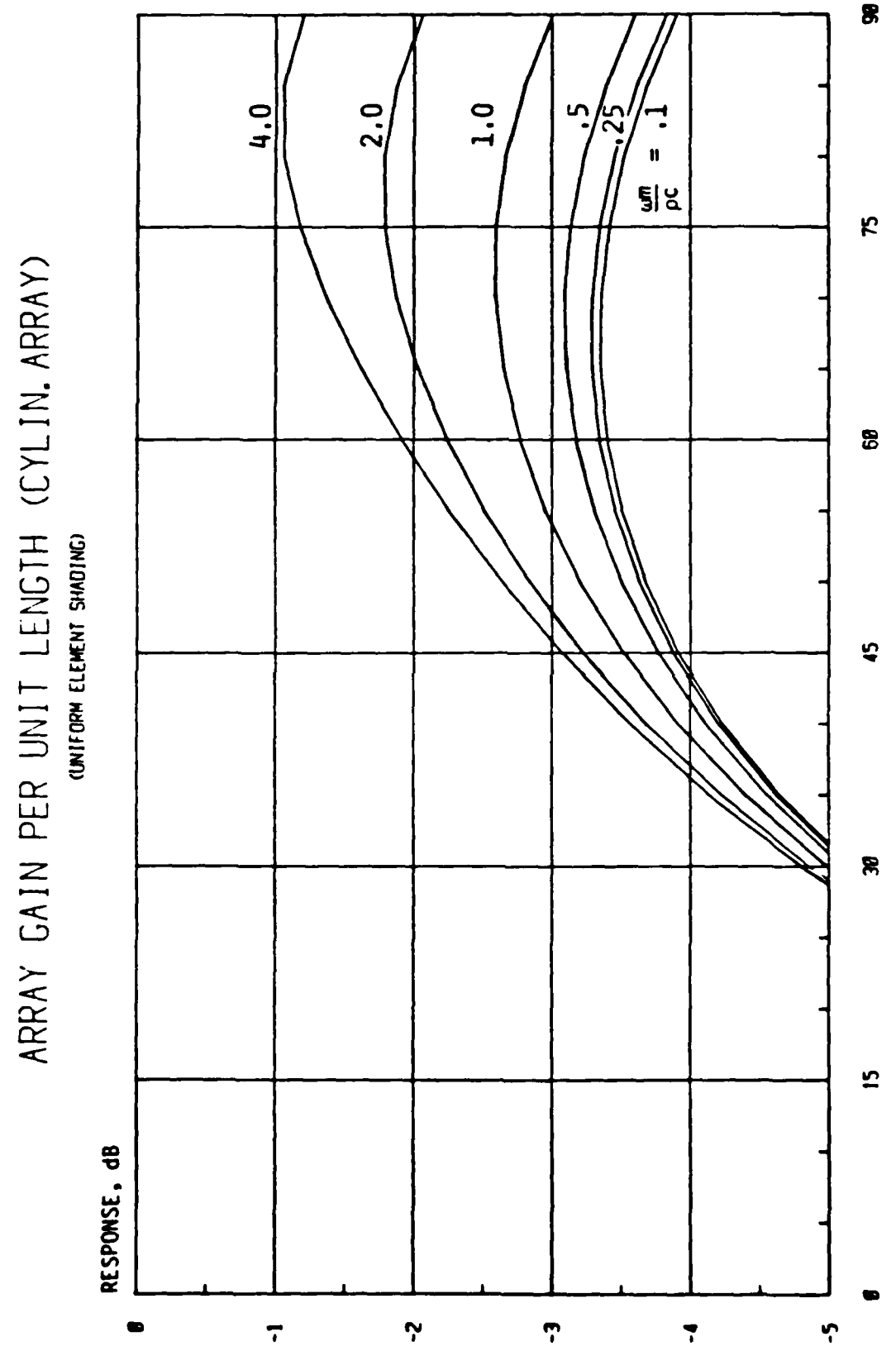

FIGURE 9 Normalized Array Gain Per Unit Length Uniform Shading

3.2 Spherical Array

The geometry of an aperture in the form of a spherical cap is illustrated in Figure 10. The cap covers the zone $\theta \leq \theta_M$. The signal arrives from $\theta = 0$. The noise is again assumed to be spatially uncorrelated.

We assume that the element directivities are symmetric about normal incidence. The array gain is

$$G(\theta_M) = \frac{2\pi R^2 \left[\int_0^{\theta_M} a(\theta)\, b(\theta) \sin\theta \, d\theta \right]^2}{\int_0^{\theta_M} a^2(\theta)\, N(\theta) \sin\theta \, d\theta} \qquad (12)$$

which corresponds to Eq. (7) for the cylindrical case.

For uniform shading ($a(\theta) = 1$) and uniform uncorrelated noise ($N(\theta) = 1$), Eq. (12) reduces to

$$G_u(\theta_M) = \frac{2\pi R^2 \left[\int_0^{\theta_M} b(\theta) \sin\theta \, d\theta \right]^2}{1 - \cos\theta_M} \qquad (13)$$

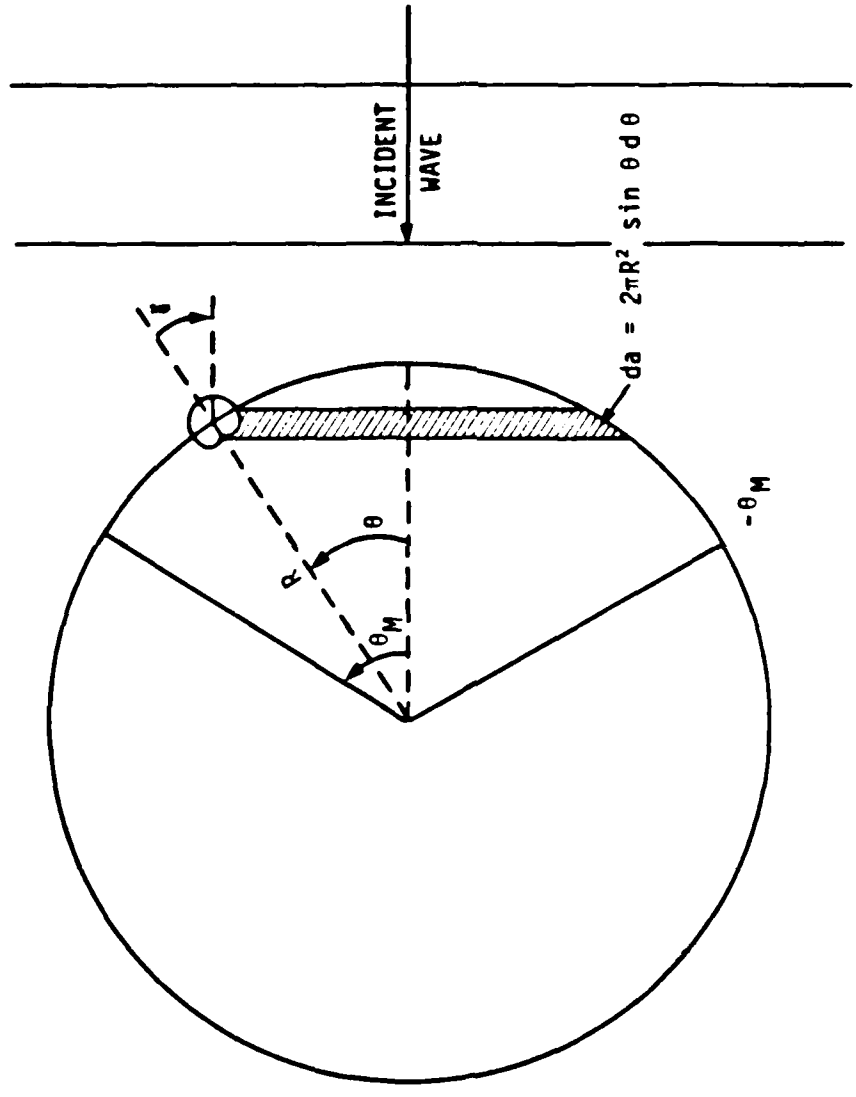

FIGURE 10 Spherical Geometry

which is analogous to Eq. (8) in the cylindrical case.

Using the Eckart shading for $N(\theta) = 1$ yields the optimum array gain

$$G_o(\theta_M) = 2\pi R^2 \int_0^{\theta_M} b^2(\theta) \sin\theta \, d\theta \tag{14}$$

which is analogous to Eq. (11) in the cylindrical case.

Using the relationship

$$\int_0^{\theta_M} \cos^n\theta \, \sin\theta \, d\theta = \frac{1 - \cos^{n+1}\theta}{n+1}, \quad n \neq -1 \tag{15}$$

it is simple to obtain closed form expressions for array gain of Equations (13) and (14) for element directivities of the cosine and cardiod family. Let

$$b(\theta) = \cos^m(\theta)$$

Then Eq. (13) becomes

$$G_u(\theta_M) = \frac{2\pi R^2}{1 - \cos\theta_M} \left[\frac{1 - \cos^{m+1}\theta_M}{m+1}\right]^2 \tag{16}$$

and Eq. (14) becomes

$$G_o(\theta_M) = 2\pi R^2 \left[\frac{1 - \cos^{2m+1}\theta_M}{2m + 1} \right] \tag{17}$$

The omnidirectional case $b(\theta) = 1$ is the special case n=0 when Equations (16) and (17) are identical

$$G(\theta_M) = 2\pi R^2 \left[1 - \cos \theta_M\right] \tag{18}$$

In this case the maximum gain is $2\pi R^2$ achieved when the full hemisphere is used as the aperture.

The cardiod and $(\text{cardiod})^2$ element directivities are easily handled by repeated application of Eq. (15). The results for $b(\theta) = (1 + \cos\theta)/2$ are:

$$G_u(\theta_M) = 2\pi R^2 \left\{(1 - \cos\theta_M)(3 + \cos\theta_M)^2/16\right\} \tag{19}$$

and

$$G_o(\theta_M) = 2\pi R^2 \left\{ \tfrac{1}{4}(1 - \cos\theta_M) + \tfrac{1}{4}(1 - \cos^2\theta_M) + \tfrac{1}{12}(1 - \cos^3\theta_M) \right\} \quad (20)$$

Similarly for $b(\theta) = (1 + \cos\theta)^2/4$

$$G_u(\theta_M) = \frac{2\pi R^2}{1 - \cos\theta_M} \left[\tfrac{1}{4}(1 - \cos\theta_M) + \tfrac{1}{4}(1 - \cos^2\theta_M) + \tfrac{1}{12}(1 - \cos^3\theta_M) \right]^2 \quad (21)$$

and

$$G_o(\theta_M) = \frac{\pi R^2}{8} \left\{ 6.2 - \left[\cos\theta_M + 2\cos^2\theta_M + 2\cos^3\theta_M + \cos^4\theta_M + \tfrac{1}{5}\cos^5\theta_M \right] \right\} \quad (22)$$

Figures 11 to 14 present normalized array gain

$$10 \log \left[G(\theta_M)/2\pi R^2 \right]$$

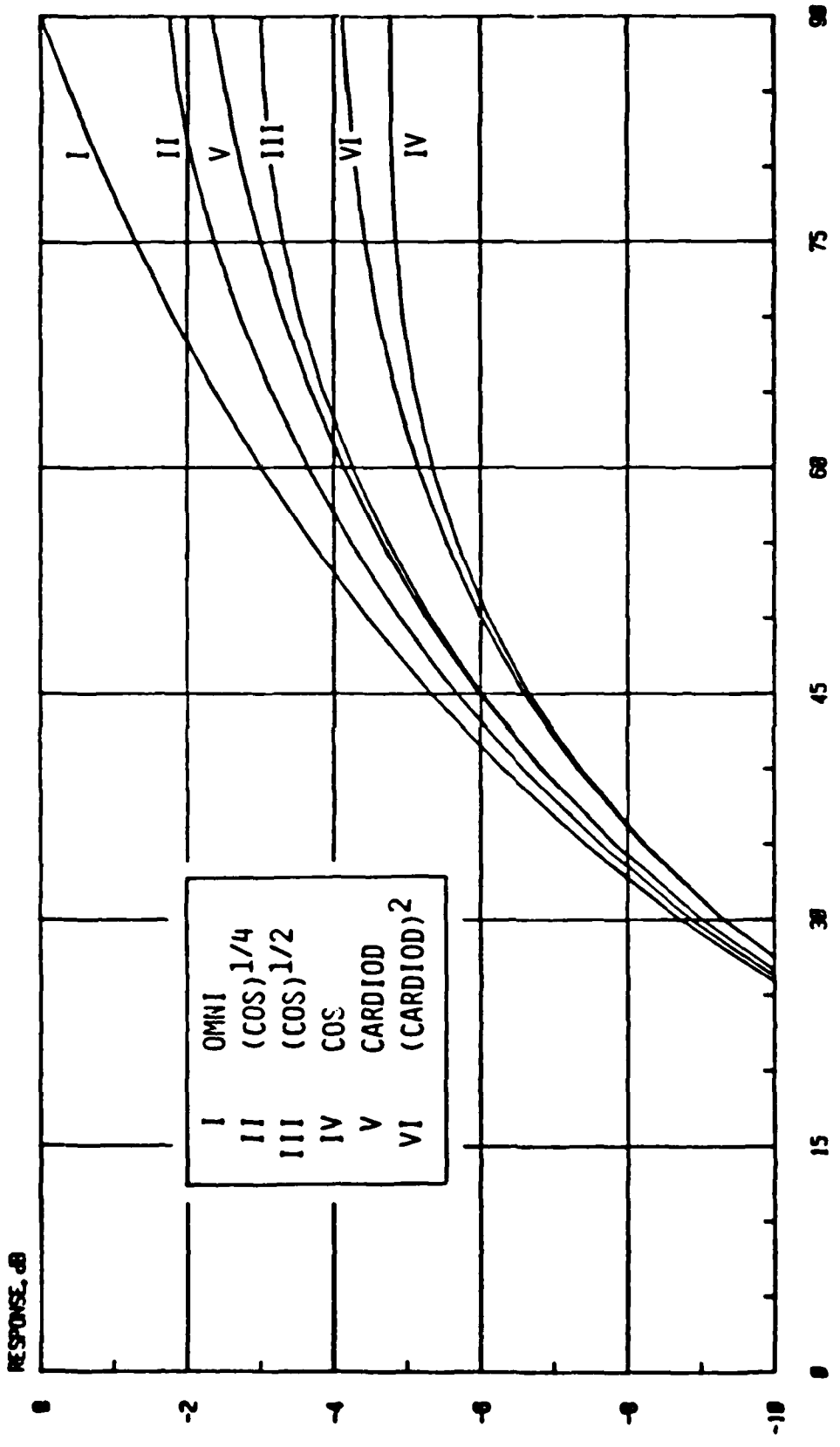

FIGURE 11 Normalized Array Gain for Spherical Cap with Optimum Shading and Various Element Directivities

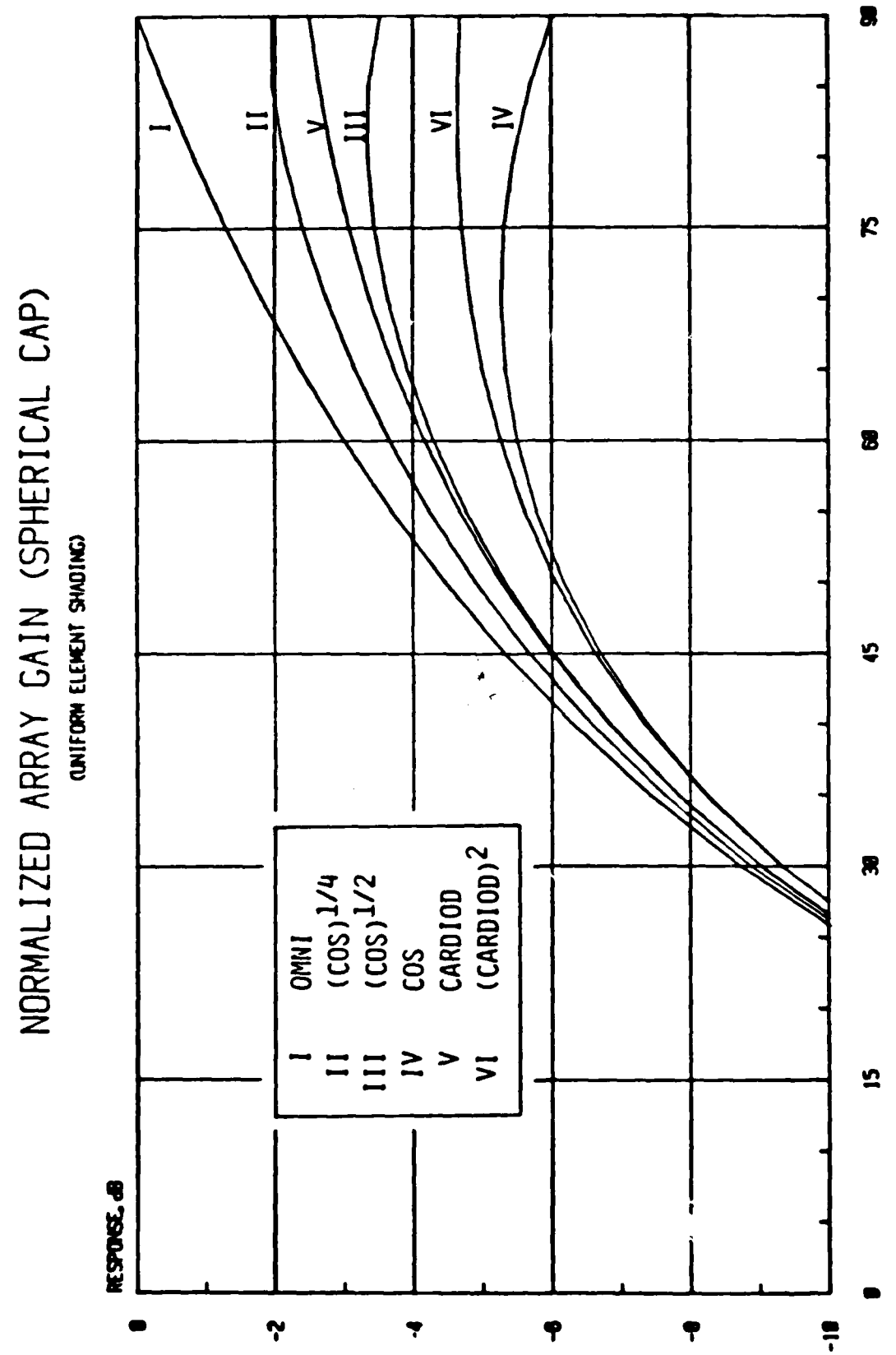

FIGURE 12 Normalized Array Gain for Spherical Cap with Uniform Shading and Various Element Directivities

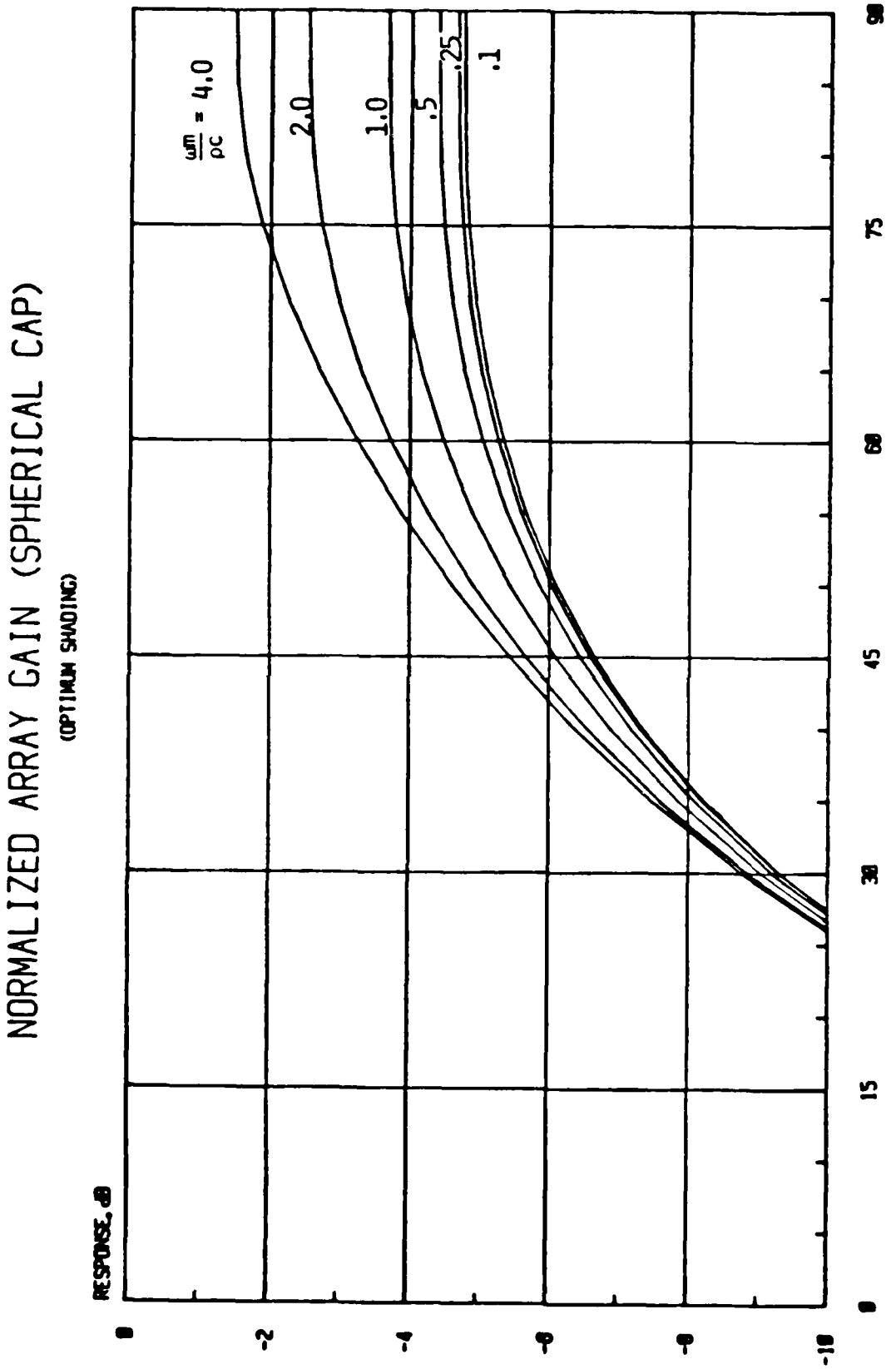

FIGURE 13 Normalized Array Gain for Spherical Cap with Optimum Shading and "Flat Plate" Element Directivities

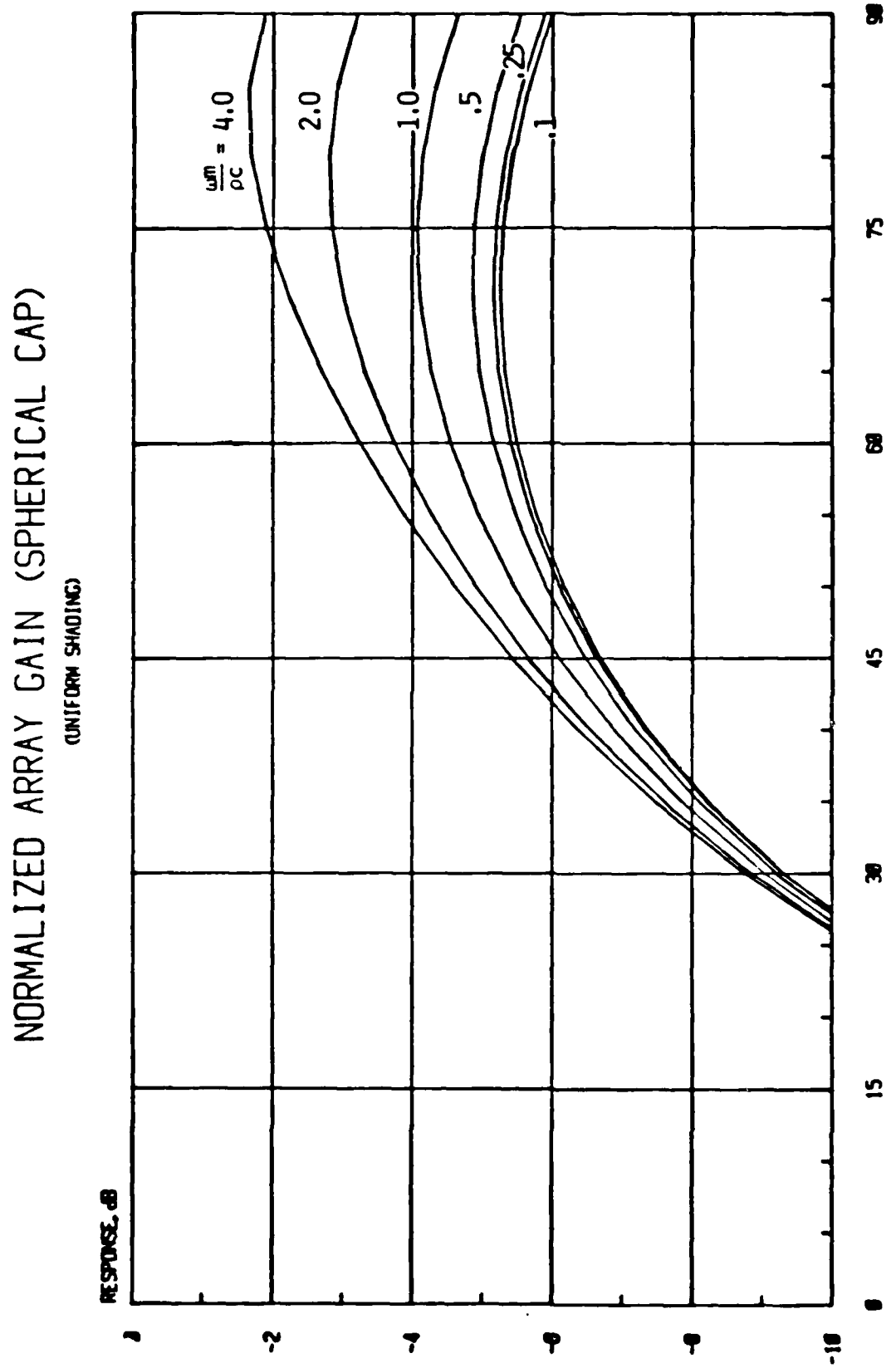

FIGURE 14 Normalized Array Gain for Spherical Cap with Uniform Shading and "Flat Plate" Element Directivities

For small aperture angles the gain increases by 6 dB for each doubling of θ_M. This compares to the increase in gain per unit length for the cylinder of 3 dB per doubling of θ_M. While the curves of Figures 11 to 14 are similar to Figures 6 to 9, it is important to notice the change in vertical scale.

Figure 11 presents results for the cosine and cardiod family of element directivities when optimum shading is used on a spherical cap. At $\theta_M = 90^\circ$, the gain for cosine directivity is about 5 dB below that for omnidirectional directivity. Increasing θ_M from 60° to 90° increases gain by 3 dB for the omnidirectional elements but by less than 1 dB for cosine directivity. The curves of Figure 11 have nearly the same shapes as those of Figure 6. Taking into account the different vertical scales, we conclude that there is about twice the payoff in increasing the aperture angle for the sphere as there is for the cylinder. This is obviously due to the increase of both the horizontal and vertical dimension of the aperture with aperture angle.

Figure 12 presents the corresponding results for uniform shading. Here we see a loss in gain for cosine directivity when θ_M is increased beyond 70°.

Figure 13 and 14 present corresponding results for "flat plate" element directivities.

In general we see more payoff in increasing aperture angle for the sphere than for the cylinder. This was expected. In a practical system design it may be desirable to use the sphere over a wider range of azimuthal angles than depression/elevation angles. In this case it may be most cost effective to truncate the array near the top and bottom allowing greater azimuthal aperture than vertical aperture. This would allow maximum gain from elements which are required for various signal directions without incurring the additional expense of adding elements which would only be used near grazing incidence.

4. SUMMARY AND CONCLUSION

When receiving arrays are placed on air backed structures in water, the effect of the structure or baffle is to alter the response of the hydrophones from their free field characteristics. The exact response characteristics are complicated and frequency dependent. Typically the response is reduced near grazing incidence. When a beam is formed for maximum response in a selected direction, increasing the aperture to include elements for which the selected beam direction is near grazing is inefficient in increasing array signal gain and may actually lead to a loss in signal-to-noise ratio. The array gain dependence upon aperture angle for cylindrical and spherical arrays has been presented for parametric families of effective element directivities. Both uniform and optimum shadings have been considered. Results have been presented in the form of parametric curves which can be used in system design tradeoffs. These results may be used to fit structural analyses and experimental data for various ACSAS candidate designs.

The use of elements when their signal response is low such as near grazing incidence has been shown to provide little additional gain against flow noise. For the cylindrical array it has been found that increasing the aperture angle beyond about 120 degrees provides less than 1 dB additional gain. Therefore economic and other system considerations such as D/E steering should be the primary factors in extending the aperture beyond 120°.

For the spherical array increasing aperture angle has about twice the payoff as for the cylindrical array since both azimuthal and vertical resolution depend on the aperture angle. Of course twice a small number may be still very small. In practice since the sphere may be used over a wide range of azimuths and must have elements for those azimuths, it may be desirable to take advantage of those elements by increasing the aperture in the horizontal dimension without adding elements near the top and bottom.